Red-Shifted Voltage-Sensitive Fluorescent Proteins

Amelie Perron,[1,3] Hiroki Mutoh,[1,3] Thomas Launey,[2] and Thomas Knöpfel[1,*]
[1]Laboratory for Neuronal Circuit Dynamics
[2]Launey Research Unit
RIKEN Brain Science Institute, Wako-shi, Saitama 351-0198, Japan
[3]These authors contributed equally to this work
*Correspondence: tknopfel@brain.riken.jp
DOI 10.1016/j.chembiol.2009.11.014

SUMMARY

Electrical signals generated by nerve cells provide the basis of brain function. Whereas single or small numbers of cells are easily accessible using microelectrode recording techniques, less invasive optogenetic methods with spectral properties optimized for in vivo imaging are required for elucidating the operation mechanisms of neuronal circuits composed of large numbers of neurons originating from heterogeneous populations. To this end, we generated and characterized a series of genetically encoded voltage-sensitive fluorescent proteins by molecular fusion of the voltage-sensing domain of Ci-VSP (*Ciona intestinalis* voltage sensor-containing phosphatase) to red-shifted fluorescent protein operands. We show how these indicator proteins convert voltage-dependent structural rearrangements into a modulation of fluorescence output and demonstrate their applicability for optical recording of individual or simultaneous electrical signals in cultured hippocampal neurons at single-cell resolution without temporal averaging.

INTRODUCTION

One of the most outstanding challenges of life sciences is to unravel the operation of complex neuronal networks in the mammalian brain. Patterns of electrical activity in large populations of nerve cells such as coherent oscillations and chains of synchronous firing (Buzsaki and Draguhn, 2004; Buzsaki, 2004; Cossart et al., 2005) cannot be investigated at the single-cell level. Unraveling such population activities requires an experimental method allowing for noninvasive and simultaneous recordings of electrical activity from large populations of selected cells of known identity. This premise motivated the development of fluorescent protein-based reporters for membrane potential (Knöpfel et al., 2006; Perron et al., 2009).

The design of first-generation genetically encoded voltage indicators was based on fusions between naturally occurring voltage-dependent ion channels and fluorescent proteins (Siegel and Isacoff, 1997; Sakai et al., 2001; Ataka and Pieribone, 2002). A subsequent more advanced second generation of probes exploited the voltage-sensing domain of the non-ion-channel protein *Ciona intestinali*s voltage sensor-containing phospha-

tase (Ci-VSP) (Murata et al., 2005) leading to sensors, termed VSFP2s (voltage-sensitive fluorescent proteins), with improved targeting to the cell surface and reliable responsiveness to membrane potential signaling in mammalian cells (Dimitrov et al., 2007; Lundby et al., 2008; Tsutsui et al., 2008; Mutoh et al., 2009). Whereas VSFP2s were designed to utilize FRET as a reporting mechanism for protein conformational rearrangements, an alternative scaffold, termed VSFP3.1, employs a voltage-dependent modulation in the fluorescence intensity of a monochromatic FP reporter (Lundby et al., 2008).

Development of next-generation voltage reporters with higher sensitivity, faster kinetics, and optimized spectral properties is nonetheless highly desirable and likely to be achievable. Further progress requires reverse engineering in order to clarify the voltage-sensing mechanism of existing prototypic probes and forward engineering based on structure-function information and newly available fluorescent reporter proteins.

Elucidating the structure of voltage-gated ion channels and relating this information to voltage-sensing mechanisms have been ambitious goals over the last several decades. Recent progress in this field resulted from the investigation of the voltage-dependent phosphatase Ci-VSP, whose voltage sensor domain is devoid of several complications associated with multi-unit voltage-gated ion channels due to its self-contained properties (Murata et al., 2005; Kohout et al., 2008). In particular, the voltage-sensing domain of Ci-VSP was shown to undergo a biphasic conformational rearrangement (Villalba-Galea et al., 2008) which correlates with the fast and slow fluorescence response component of Ci-VSP-based fluorescent voltage reporters (Lundby et al., 2008; Mutoh et al., 2009; Villalba-Galea et al., 2009).

Forward engineering of FP-based sensors is further facilitated by a large body of structural and photophysical knowledge related to new and improved versions of *Aequorea victoria* GFP and GFP-like proteins (Verkhusha and Lukyanov, 2004; Shaner et al., 2007; Pakhomov and Martynov, 2008). In particular, great efforts have been focused on developing and characterizing monomeric variants of orange- and red-emitting FPs derived from *Discosoma* sp. and *Enctacmaea quadricolor*, namely mOrange2 (Shaner et al., 2008), TagRFP (Merzlyak et al., 2007), and mKate (Shcherbo et al., 2007, 2009). These are of particular interest, as far-red fluorescence provides better spectral separation from green tissue autofluorescence in addition to larger effective light penetration for deep tissue imaging using two-photon excitation microscopy.

Herein, we took advantage of these newly available FPs with particular emphasis on red-shifted variants to spectrally tune

our VSFP3.1 sensor by generating a new series of mono-chromatic FP-based voltage-sensitive probes with spectral variants spanning the yellow to far-red region of the visible light spectrum. These color variants exhibited distinct voltage-sensing properties which could be explained by a different contribution of the fast versus slow kinetic components associated with their fluorescence response. Testing of the most promising VSFP3.1 variant in hippocampal neurons showed reliable report of individual and simultaneous electrical signals at the single-cell level without temporal averaging. Most importantly, this study establishes a conceptual platform for directed development of enhanced VSFPs based on mono-chromatic FPs.

RESULTS

Design and Generation of VSFP3.1 Spectral Variants

VSFP3.1 was originally obtained by deleting the acceptor chromophore from the cyan/yellow-emitting VSFP2.1 voltage sensor to take advantage of a FRET independent component in its voltage-sensing response (Lundby et al., 2008) (Figure 1A). Although this new scaffold offered the promise of fast fluorescence readouts, the voltage-sensing mechanism of this monochromatic reporter protein remained unknown. Furthermore, the photophysical properties of Cerulean are less than ideal for live-cell fluorescence imaging due to its low fluorescence quantum yield, spectral overlap with tissue autofluorescence, and low photostability (Shaner et al., 2005, 2007). In order to address these issues, we generated a new series of fusion proteins by replacing the FP reporter in VSFP3.1 with Citrine, a yellow-emitting variant of *A. victoria* GFP with reduced sensitivity to pH (Griesbeck et al., 2001), or with bright and photostable Anthozoan GFP-like proteins emitting in the orange (mOrange2 [Shaner et al., 2008]) and red (TagRFP [Merzlyak et al., 2007] and mKate2 [Shcherbo et al., 2009]) regions of the spectrum (Figure 1B). The alignment of the amino acid sequences of the fluorescent reporter proteins used in this study is illustrated in Figure S1 available online.

Expression and Voltage-Sensing Response of VSFP3.1 Color Variants in PC12 Cells

The newly generated VSFP3.1 spectral variants were first examined for their distribution pattern in transfected PC12 cells by confocal fluorescence microscopy. As illustrated in Figure 2A, all of the constructs were found to be both fluorescent and targeted to the plasma membrane, albeit with different efficiencies. Most notably, VSFP3.1_mOrange2 and VSFP3.1_mKate2 displayed bright fluorescence with prominent targeting to the plasma membrane. Similarly, VSFP3.1_Citrine and VSFP3.1_TagRFP were largely found at the cell surface, together with a small intracellular fluorescence component associated with a juxtanuclear structure as observed with the original Cerulean-based VSFP3.1.

Each of the new constructs was then tested for the modulation of their fluorescence output upon depolarization in transfected PC12 cells. As shown in Figure 2B, all VSFP3.1 spectral variants were voltage sensitive and exhibited a biphasic decrease in their fluorescence yields in response to depolarizing test potentials, as previously reported for VSFP3.1 (Lundby et al., 2008).
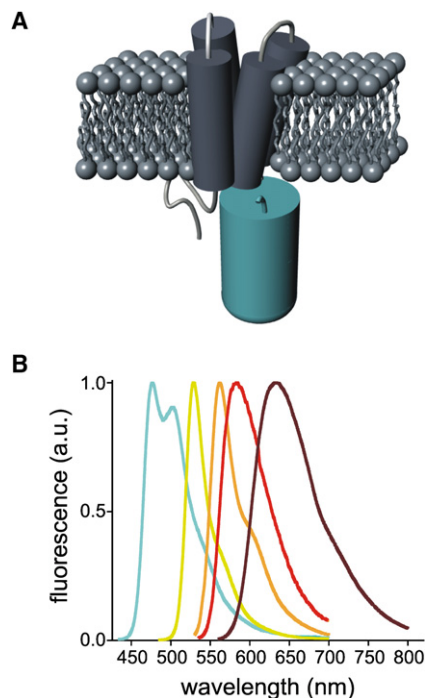

Figure 1. Conceptual Design of VSFP3.1-Based Voltage-Sensitive Probes

(A) Schematic representation of the VSFP3.1 original prototype wherein a cyan-emitting FP is attached to the VSD of Ci-VSP.

(B) Emission spectra of the fluorescent reporter proteins used to generate the VSFP3.1 spectral variants. Curves are shown with a color corresponding to each spectral variant: Cerulean (cyan), Citrine (yellow), mOrange2 (orange), TagRFP (red), and mKate2 (burgundy). The emission spectra of Cerulean, Citrine, and mOrange2 were taken from the Tsien lab website (http://www.tsienlab.ucsd.edu/documents.htm). TagRFP and mKate2 emission spectra were obtained from the Evrogen website (http://www.evrogen.com).

Kinetics of Voltage-Dependent Fluorescence Signals

The kinetic properties of VSFP3.1 spectral variants were then thoroughly investigated with a standardized voltage-clamp protocol and analysis scheme as illustrated for VSFP3.1_mOrange2 in Figure 3. Membrane voltage was stepped from a holding level of -70 mV to test potentials ranging from -140 to 60 mV in 40 mV increments (Figure 3A). Analysis of averaged fluorescence transients indicated that both ON (onset of response to voltage change) and OFF (return to baseline levels) responses could not be accurately approximated by a single exponential fit but were well fitted with a double exponential function to the first 150 ms following the change in command potential (Figure 3B). Time constants corresponding to the fast and slow components associated with the ON and OFF responses were plotted as a function of step voltage as shown in Figures 3C and 3E, respectively. Fitting of these curves with Boltzmann functions revealed the half-maximal response potential ($V_{1/2}$) for the fast, slow, and total components of the fluorescence signal (Figures 3D and 3F). Interestingly, the fast ON time constant displayed a clear maximum around $V_{1/2}$, consistent with the notion that it is directly reporting the voltage-dependent charge displacement (sensing currents) within the VSD (Villalba-Galea et al., 2008, 2009). Furthermore, the slow OFF time component was rather
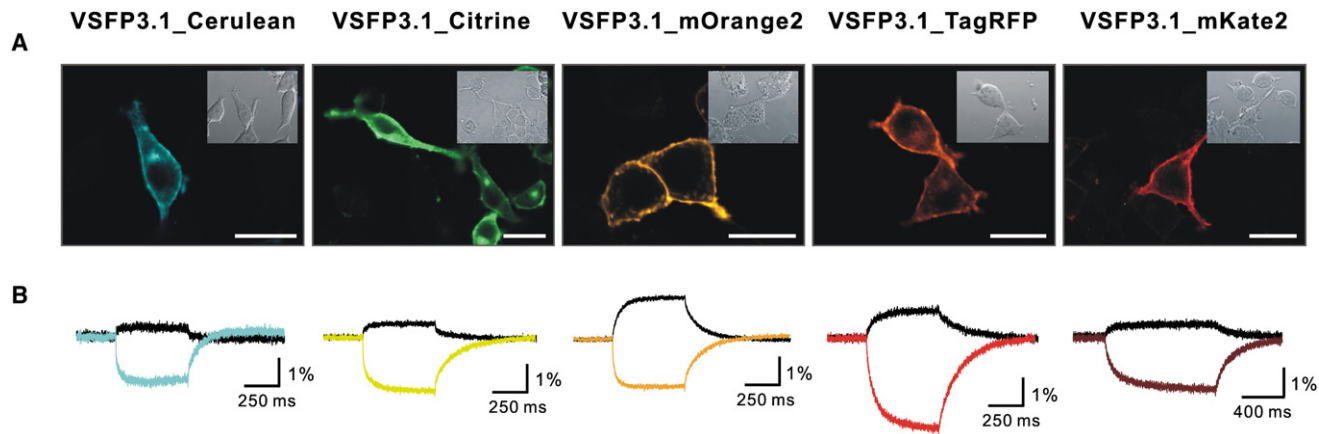
Figure 2. Expression and Voltage-Sensing Characteristics of VSFP3.1 Color Variants in PC12 Cells

(A) Fluorescence and transmission images of PC12 cells expressing VSFP3.1_Cerulean, VSFP3.1_Citrine, VSFP3.1_mOrange2, VSFP3.1_TagRFP, and VSFP3.1_mKate2. Scale bars indicate 20 μm.

(B) Fluorescence signals in response to test potentials of −140 to 60 mV from a holding potential of −70 mV at 35°C.

insensitive to membrane voltage, as expected from its role in tracking the voltage-independent relaxation of the activated VSD (Villalba-Galea et al., 2008, 2009). Likewise, voltage-clamp fluorometric measurements were conducted for VSFP3.1_Cerulean (Figure S2), VSFP3.1_Citrine (Figure S3), VSFP3.1_TagRFP (Figure S4), and VSFP3.1_mKate2 (Figure S5), and calculated parameters for ON and OFF response properties are summarized in Table 1 and Table S1, respectively.

This analysis indicated that the response kinetics of the VSFP3.1 color variants could be described by relatively similar ON and OFF time constants as well as comparable $V_{1/2}$ values. However, the spectral variants exhibited clear differences in the relative contribution of the fast and slow components associated with their ON and OFF time fluorescence readouts. As detailed in the Discussion, these two response components correspond to two distinct structural transitions within the VSD of Ci-VSP.

Voltage-Dependent Modulation of Fluorescence Is Not Caused by Depolarization-Induced pH Changes

Changes in membrane potential can cause changes in local pH and, indeed, physiological pH changes might become problematic for the interpretation of signals from GFP-derived sensors (Kneen et al., 1998). This issue might particularly be important for fluorescent proteins with a pK_a close to physiological values, which could possibly report pH-dependent fluctuations in absorption and quantum yield rather than depolarization-induced conformational changes. In order to clarify that the fluorescent signal observed with VSFP3.1-based sensors is caused by voltage-dependent structural rearrangements in the VSD rather than local pH changes, we generated a VSFP3.1-mOrange2 variant wherein the neutral glutamine at position 217 of the VSD was reversed to the native arginine (Q217R). We previously showed that this mutation causes a rightward shift of the voltage-activity curve to positive values (Dimitrov et al., 2007). We decided on mOrange2 as a fluorescent reporter protein for this voltage-shifted sensor because its pK_a value (6.5; Shaner et al., 2008) is the highest among the FP selected

in this study. As shown in Figure 4, VSFP3.1_mOrange2(R217Q) and VSFP3.1_mOrange2(Q217R) exhibited different fluorescence responses to test potentials. Indeed, VSFP3.1_mOrange2(Q217R) (Figure 4B) did not show any change in fluorescence for voltage values lower than the holding potential (−70 mV), whereas VSFP3.1_mOrange2(R217Q) (Figure 4A) showed a clear increase in fluorescence intensity for −100 and −140 mV step potentials. In addition, VSFP3.1_mOrange2(Q217R) fluorescence did not reach a plateau at 20 mV (as opposed to VSFP3.1_mOrange2[R217Q]) but kept on decreasing until 100 mV (Figure 4C), indicating that the fluorescence signal of mOrange2 reflects the voltage-dependent structural rearrangement of the VSD rather than voltage-dependent fluctuations in local pH, which should not be affected by the Q217R point mutation. Furthermore, a similar voltage-clamp protocol carried out in PC12 cells loaded with SNARF, a fluorescent pH indicator, did not resolve any changes in intracellular pH during the 500 ms depolarizing pulses under our recording conditions (data not shown).

Performance of Probes for Optical Recordings of Neuronal Electrical Activity

The primary purpose of this study was to shed light on the mechanism of monochromatic FP voltage-sensitive probes and to expand the spectral range of the currently available VSFPs. As a result of this work, we generated several promising new membrane voltage reporters. To evaluate the potential of these probes for optical recordings of neuronal activity, we first validated the expression pattern of VSFP3.1_Citrine, VSFP3.1_TagRFP, VSFP3.1_mKate2, and VSFP3.1_mOrange2 in transfected neurons from mouse hippocampal cultures. As shown in Figure 5, confocal fluorescence imaging revealed that the fluorescence of these red-shifted VSFP3.1 voltage sensors was distributed over the cell body, dendrites, and axons of a variety of neurons including pyramidal cells. It was also evident that their brightness and contrast against intrinsic background autofluorescence was significantly higher than what was previously reported for the Cerulean-based VSFP3.1 prototype
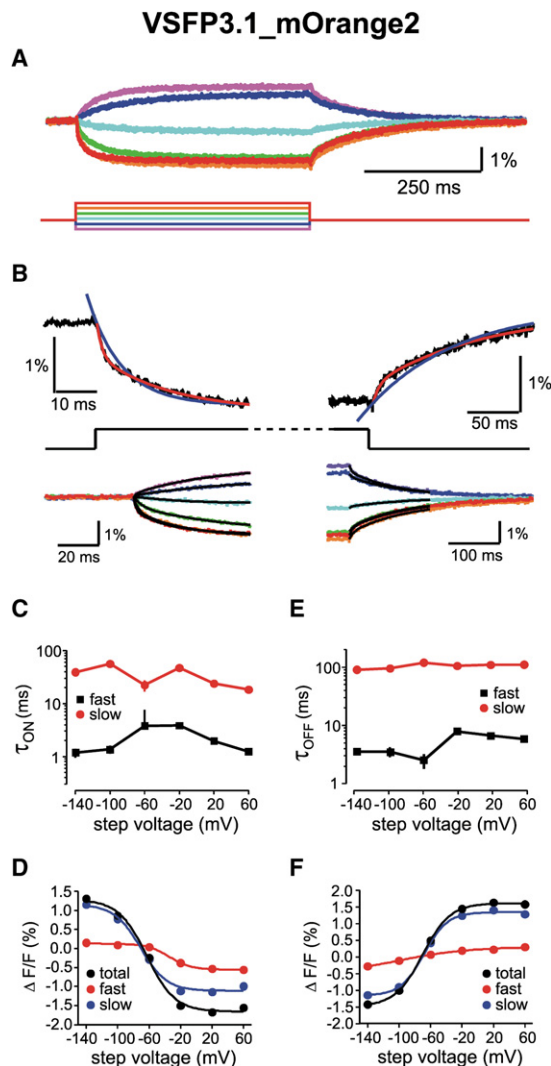
VSFP3.1_mOrange2

Figure 3. Analysis of VSFP3.1_mOrange2 Kinetic Properties

(A) Fluorescence signals (upper panel) evoked by a family of voltage steps from −70 mV to step potentials ranging from −140 to 60 mV in 40 mV increments (lower panel).

(B) ON (left panel) and OFF (right panel) responses (black traces) were well fitted by two exponentials (red), whereas a single exponential (blue) did not yield satisfactory fits. Lower panels show the double exponential fits of the ON (left) and OFF (right) time components of the fluorescence signal in response to each command potential.

(C–F) Voltage dependence for the fast and slow time constants of the ON (C) and OFF (E) responses. Voltage dependence of fluorescence yields for the fast and slow components and total amplitude of ON (D) and OFF (F) responses. Data represent averages over 11 cells of 6–12 consecutive sweeps of the voltage step protocol. Fit errors are indicated by vertical bars in (C) and (E) and are omitted for clarity in (D) and (F).

(Perron et al., 2009). As in PC12 cells, VSFP3.1_mOrange2 (Figure 5D), VSFP3.1_TagRFP (Figure 5B), and VSFP3.1_mKate2 (Figure 5C) exhibited efficient targeting to the plasma membrane. Although VSFP3.1_mCitrine (Figure 5A) fluorescence was mainly found at the cell surface, some fluorescence was also evident intracellularly within a perinuclear structure, as observed with VSFP3.1_Cerulean (Perron et al., 2009).

A critical benchmark for a voltage-sensitive fluorescent probe suitable for the investigation of neuronal circuit function is its ability to resolve activity at the single-cell level without averaging over repetitive time sweeps. Based on its advantageous spectral properties, high dynamic range of its fluorescence signal, and relatively fast response kinetics (Table 1; Table S1), we chose VSFP3.1_mOrange2 for this benchmark experiment. Hippocampal VSFP3.1_mOrange2-expressing neurons were patch clamped so that their electrical activity could be monitored by a microelectrode simultaneously with the optical recordings. Hippocampal neurons grown in dissociated cultures are known to develop intrinsic network activity characterized by a high rate of synchronized events after 7 days in vitro (Cohen et al., 2008). As illustrated in Figure 5E, VSFP3.1_mOrange2 clearly reported spontaneous bursting activities (upper traces, Figure 5E), but also synaptic events underlying single action potentials (asterisks, lower traces, Figure 5E). Among these membrane potential fluctuations, the optical signal showed deflections that were larger with action potential bursts but are still resolvable in a single sweep even when the supra-threshold depolarizations trigger only one action potential. As expected from the prevalence of the slower component of the VSFP3.1_mOrange2 voltage response, these optical signals predominantly reflected slow voltage transients associated with synaptic event rather than the time course of fast action potentials. Notably, cortical cells recorded in living animals exhibit spontaneous activities reflecting either intrinsic network dynamics or sensory-induced responses that comprise similar slow synaptically triggered membrane depolarization events which eventually trigger action potentials (see, e.g., Manns et al., 2004; Crochet and Petersen, 2006). Because of the relatively small contribution of the faster VSFP3.1_mOrange2 response time constant, this probe efficiently reports subthreshold membrane potential fluctuations and, accordingly, provides a readout complementary to that obtained with calcium-sensitive dyes which preferentially report action potential spiking activities. For experiments where a separation of action potentials from slower synaptically driven voltage transients is desirable, VSFP3.1_Cerulean may be an alternative choice, as this voltage probe variant's fast response time constant predominates over its slower counterpart. However, this variant is not red shifted.

To verify that these optical signals are detectable with spatial resolution, we used an imaging system comprising a CCD camera mounted on an inverted microscope for fluorescence detection. In this set of experiments, we imaged fields of view from hippocampal cultures containing several transfected neurons wherein one of them was patch clamped to record spontaneous electrical activity. In the example shown in Figure 6, a patch-clamped neuron expressing VSFP3.1_mOrange2 (see position of electrode in Figure 6A, upper panel) exhibited large spontaneously occurring excitatory synaptic potentials resulting in one or two action potentials. Fluorescence time course traces sampled over the soma of the cell (area of interest 1, Figure 6A) demonstrated a strong correlation with the microelectrode signals (Figures 6B–6D). Similar responses were also observed in the optical signals sampled from distal dendritic branches (area of interest 2, Figure 6A), highlighting the feasibility of recording optical signals from cellular compartments that are

Table 1. Summary of ON Time Response Properties of VSFP3.1 Spectral Variants

Color Variant	Fast τ_{ON}[a] at −20 mV (ms)	$V_{1/2}$[b] Fast τ_{ON} (mV)	Slow τ_{ON}[a] at −20 mV (ms)	$V_{1/2}$[b] Slow τ_{ON} (mV)	Fast/Slow (%)	$V_{1/2}$[b] Total τ_{ON} (mV)	Dynamic Range (%)
Cerulean	1.8 ± 0.3	−34.7 ± 3.6	77.5 ± 34	−49.2 ± 10.8	69	−43.6 ± 5.4	1.9
Citrine	2.2 ± 0.2	−21.2 ± 2.0	81 ± 21	−48.4 ± 2.0	51.9	−40.5 ± 2.1	1.6
mOrange2	3.8 ± 0.3	−34.4 ± 3.5	47.3 ± 4.7	−70.8 ± 5.3	34	−63.0 ± 4.0	2.9
TagRFP	3.2 ± 0.6	−54.3 ± 1.7	60.9 ± 9.4	−46.1 ± 8.6	17.5	−47.3 ± 7.9	3.5
mKate2	n/a	n/a	54.3 ± 15.7	−47 ± 2	<1	−41.7 ± 2.2	1.3

[a] Optical signals were fitted with a double exponential function for at least ten cells for each variant. Resulting slow and fast time constants are given as means ± SD.
[b] $V_{1/2}$ values were fitted with a Boltzmann function and represent means ± SD of a minimum of ten cells per variant. n/a, not applicable (no fast time constant revealed).

normally difficult to access with microelectrodes. Moreover, optical signals sampled from neighboring cells (area of interest 3, Figure 6A) revealed that the spontaneous activities measured in these hippocampal cultures likely represent synchronized network activity (Cohen et al., 2008). Thus, the VSFP3.1_mOrange2 genetically encoded optical probe allows both for individual and simultaneous voltage imaging of neuronal network activities at the single- or multiple-cell optical resolution level in monolayer neuronal cultures.

DISCUSSION

By using a reverse engineering approach based on FPs with optimized photophysical properties, we have generated and characterized a novel series of red-shifted variants of VSFP3.1, the Ci-VSP-based genetically encoded voltage sensor with the fastest response kinetics reported to date (Lundby et al., 2008). All VSFP3.1 color variants were shown to convert membrane potential variations into changes in fluorescence intensity with unexpectedly different kinetics. These discrepancies could be explained by different contributions of their voltage-sensing response to the fast and slow components of a biphasic mechanism that likely reflects two major conformations in the voltage-dependent rearrangement of the VSD of Ci-VSP (Villalba-Galea et al., 2008). The most promising variant, VSFP3.1_mOrange2, was successfully benchmarked for its use as an optical reporter for neuronal activity.

Figure 4. The Voltage Dependency of mOrange2 Is Coupled to the Voltage Dependency of the VSD

(A and B) PC12 cells expressing either VSFP3.1_mOrange2(R217Q) (A) or VSFP3.1_mOrange2(Q217R) (B) were subjected to a voltage-clamp recording protocol comprising a family of 500 ms voltage steps from a holding potential of −70 mV to test potentials of −140 to 60 mV or −140 to 140 mV. Traces are averages of ten cells.

(C) Fluorescence-voltage relationship of the VSFP3.1_mOrange2-based variants. Responses were fitted to a single Boltzmann equation.

How Does the VSD Conformational State Modulate FP Output?

Monitoring membrane voltage-dependent structural rearrangements with a monochromatic FP reporter was demonstrated more than a decade ago in the case of FlaSh, a sensor derived from the fusion of GFP to the *Shaker* voltage-gated K^{+} channel (Siegel and Isacoff, 1997). Yet the mechanism by which a single FP can report conformational changes of a fusion partner has remained poorly understood. In circularly permuted FPs, the β barrel-like structure has been weakened so that the degree of collisional quenching of the chromophore is sensitive to conformational changes at the fusion interface (Baird et al., 1999; Nakai et al., 2001; Akerboom et al., 2009). This principle has been successfully exploited in fluorescent calcium indicator proteins (Baird et al., 1999; Nakai et al., 2001; Nagai et al., 2001; Souslova et al., 2007). FPs with a native β barrel structure are, however, rather resistant to forces imposed on the C or N termini forming the fusion interface. The fluorescence signals of VSFP3.1 variants are, therefore, more likely due to a displacement of the entire FP within a physicochemical gradient upon the depolarization-driven structural rearrangement within the VSD (Murata et al., 2005; Villalba-Galea et al., 2008), resulting in a change in the local environment surrounding the chromophore.
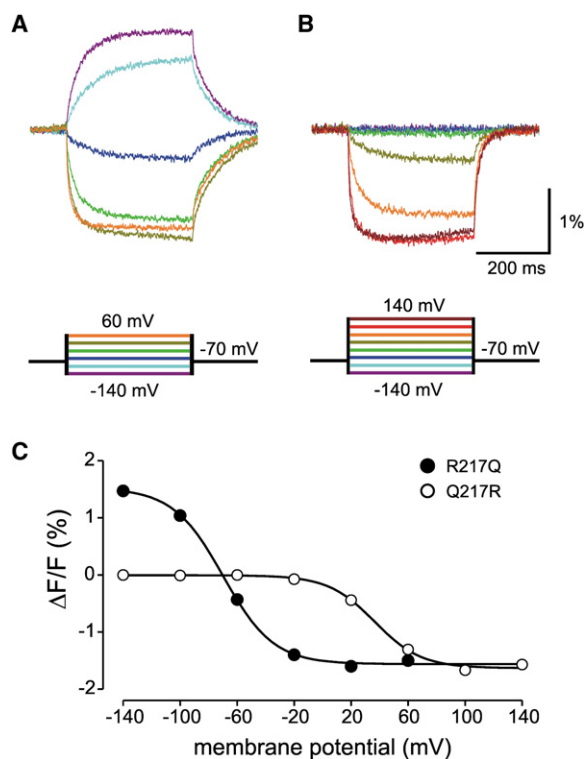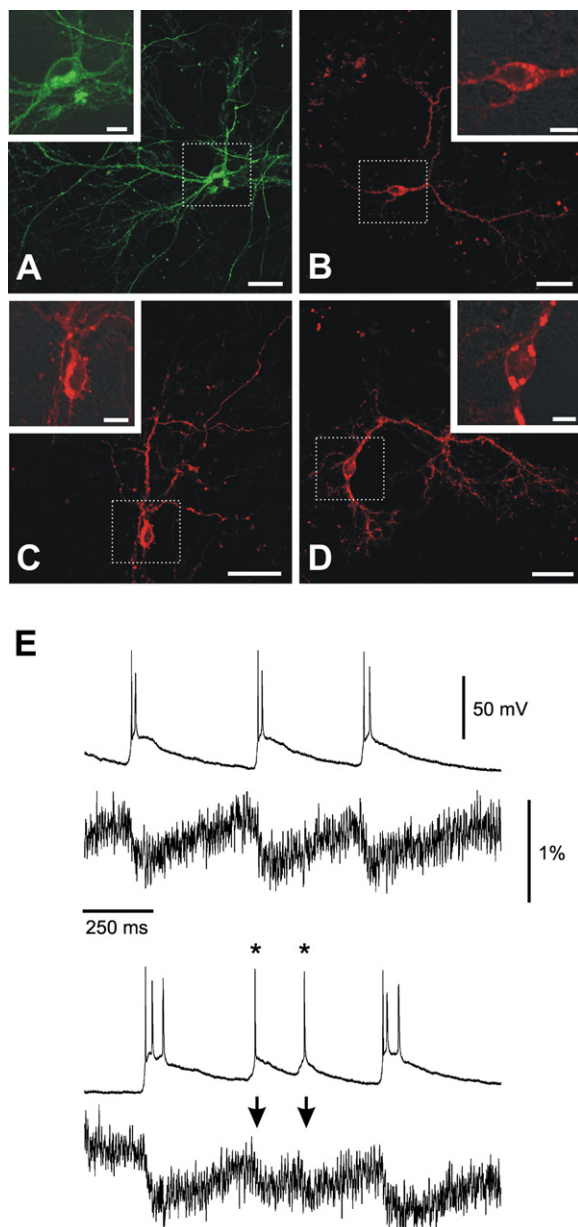
Figure 5. Expression and Functional Validation of Red-Shifted VSFP3.1-Based Voltage Sensors in Neuronal Cultures

(A–D) Confocal fluorescence imaging of primary hippocampal cultures expressing VSFP3.1_Citrine (A), VSFP3.1_TagRFP (B), VSFP3.1_mKate2 (C), or VSFP3.1_mOrange2 (D). Magnified views of boxed regions are shown in inserts. Scale bars indicate 40 μm (overviews) and 10 μm (inserts).

(E) Optical recordings of spontaneous electrical activity in primary neuronal cultures derived from mouse hippocampus. The neurons were transfected with VSFP3.1_mOrange2 and the recordings were done under current-clamp conditions at 35°C. Asterisks indicate individual action potentials that were resolved optically in single sweeps (arrows).

A similar mechanism was suggested in voltage-clamp fluorometric studies with *Shaker* potassium channels covalently labeled with the environment-sensitive fluorophore tetramethylrhodamine-6-maleimide (Mannuzzu et al., 1996; Cha and Bezanilla, 1997). Well-established physicochemical parameters

known to affect fluorescence characteristics (fluorescence intensity and/or fluorescence lifetime) of FPs include pH (Kneen et al., 1998; Llopis et al., 1998), refractive index (Suhling et al., 2002; Borst et al., 2005; van Manen et al., 2008), and membrane hydration (Verkhusha et al., 2003; Uskova et al., 2000). We, however, exclude a VSD independent, depolarization-induced cytosolic acidification as a cause for VSFP3.1 fluorescence signals, because the fluorescence readout shifted in parallel with a corresponding change in the voltage dependency of the VSD as shown for the VSFP3.1_mOrange2 variants comprising either the neutral Q217 or native R217 arginine in the VSD.

Alternatively, the emission of the FPs could also monitor a Gouy-Chapman proton gradient at the water-protein-lipid interface upon VSD-mediated translocation (Cevc, 1990). This possibility is nonetheless unlikely, given that there was no correlation between dynamic range of the fluorescence response and pK_a within the set of probes characterized in this study (Figure S6). Although the FPs likely move from a lower ($n_{cytoplasm} = 1.35$) to higher ($n_{membrane} = 1.46–1.60$) refractive index and that the fluorescence decay of FPs is known to be affected by the local refractive index (Suhling et al., 2002; Borst et al., 2005), it is, nevertheless, not known whether changes in fluorescence lifetime are associated with changes in fluorescence output of the FP species used in our study. We also exclude changes in average chromophore orientation relative to the optical axis in our measurements because our signals are spatial averages over whole cells. By exclusion of the above possibilities but without direct supportive evidence, we propose that the most conceivable mechanism underlying the voltage-dependent modulation of VSFP3.1 fluorescence is a change in hydrophobic interactions at the FP surface upon VSD-induced translocation relative to the plasma membrane. Indeed, there are several reports showing that alterations of hydrophobic interactions (e.g., during development of monomeric FP variants) can have a dramatic effect on fluorescence quantum yield (Campbell et al., 2002; Merzlyak et al., 2007). The different kinetics and dynamic range observed among the VSFP3.1 spectral variants are consistent with different dipolar and H-bonding interactions of the fluorophore with neighboring water molecules at the cytosol-lipid interface that might result in slow and small relaxations within the FP electronic structure.

What Does the Fluorescent Signal Report?

VSFP fluorescent probes respond to membrane potential indirectly by reporting voltage-dependent structural rearrangements within their VSD. Recent studies wherein florescence signals were measured simultaneously with sensing currents indicated that the fast component of the fluorescence response is related to charge displacement within the VSD of Ci-VSP, whereas the slow component represents a relaxation of the VSD during prolonged depolarization (Villalba-Galea et al., 2008, 2009). The thorough analysis of our several VSFP3.1 color variants presented here provides strong supporting evidence for this model. Importantly, the fast ON time constant showed a pronounced voltage dependency with peak values around $V_{1/2}$, as expected from a direct tracking of charge motions. In all of the variants that exhibited a pronounced fast response component (e.g., VSFP3.1_Cerulean, VSFP3.1_Citrine, and VSFP3.1_mOrange2),
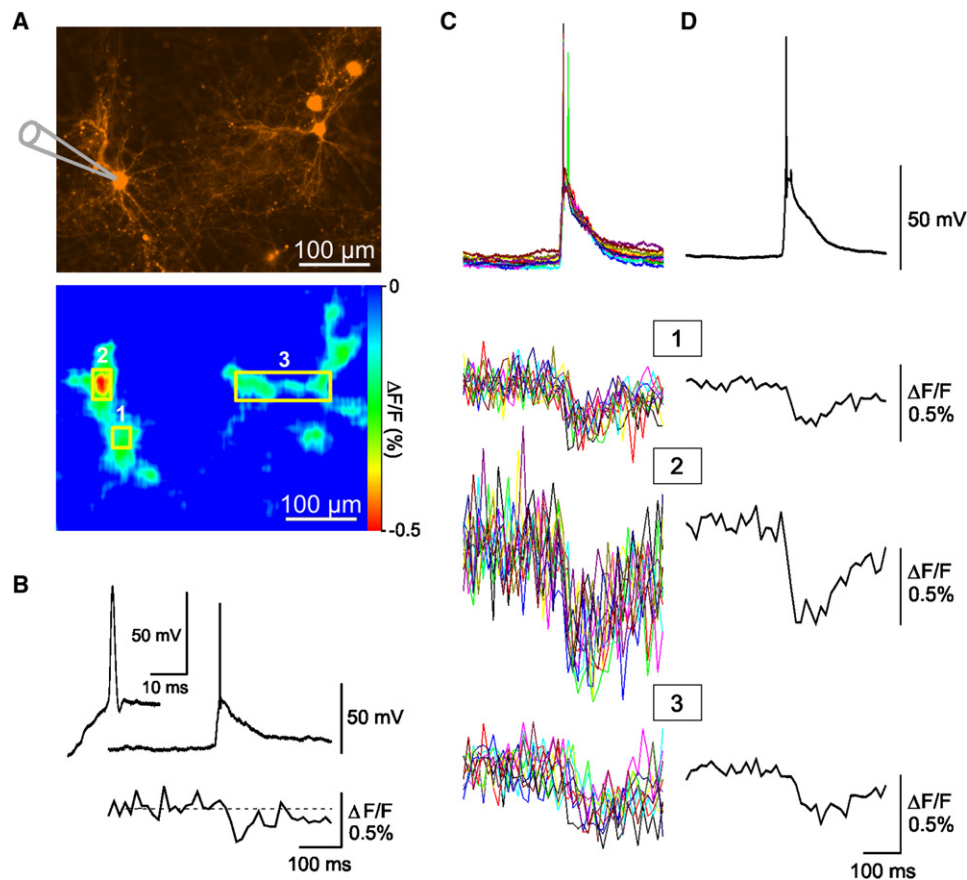
Figure 6. Optical Imaging of Electrical Activity in VSFP3.1_mOrange2-Expressing Hippocampal Neurons

(A) Upper fluorescence image shows a field of view containing several transfected neurons. The cell on the left was patch clamped (a schematic drawing shows the glass electrode) and recorded in current-clamp mode. The lower image illustrates a color-coded map of fluorescence changes during the peak of the optical signals shown in (B)–(D).

(B–D) Spontaneous synaptic potentials triggered action potential activity associated with a decrease in fluorescence. The upper and lower traces represent microelectrode and optical recordings, respectively. Traces are single sweeps taken from a region of interest (ROI; yellow rectangles) comprising the cell body of the patch-clamped neuron (ROI 1 in A). The insert shows the action potential at a magnified time scale. Superposition (C) and average (D) of single-sweep microelectrode (top traces) and optical (lower three traces) recordings are also shown. The optical recordings were obtained from ROI 1–3 as illustrated in A. Note: ROI 2 shows responses from the dendrite of the patch-clamped cell and ROI 3 illustrates a synchronized response from an adjacent cell.

the $V_{1/2}$ of the fast OFF time component was clearly shifted toward negative potentials as compared to the $V_{1/2}$ of the fast ON time component, which is consistent with a conformational change into the relaxed state proposed by Bezanilla and coworkers (Villalba-Galea et al., 2008). Interestingly, VSFP3.1_TagRFP, in which the fast ON time component was small or not resolvable, did not show this voltage shift. In addition, the contribution of the fast and slow components of the fluorescence response showed clear divergences among the VSFP3.1 spectral variants. There are at least two conceivable explanations for this: (1) different FPs affect the equilibrium between the active and relaxed state; this may account in particular for the slow kinetics of TagRFP- and mKate2-based VSFP3.1 variants; and (2) the effectiveness in tracking the two different components of the VSD depolarization-induced structural rearrangements may differ between the FPs. This is to be expected if the fluorescence signals are caused by hydrophobic interactions specific to the surface of each FP.

Finally, VSFP3.1 color variants exhibited slightly different kinetics. As discussed above, these discrepancies may reflect different conformation-dependent hydrophobic interactions of the protein matrix surrounding the chromophore with the membrane-cytosol interface. Alternatively, or in addition, the FP reporters used in this study might differently affect the kinetics of the VSD sensing mechanism. Indeed, recent work has shown that the phosphatase domain of the native Ci-VSP or FP fusion partners affects the kinetics of sensing currents (i.e., conformational changes) of the VSD by imposing a mechanical load (Villalba-Galea et al., 2008). We also noted that the dynamic range calculated from the dual exponential fits of the OFF response was slightly but consistently larger than that calculated from the double exponential fits of the ON response (Table 1; Table S1), suggesting an additional very slow "relaxation" that is not well captured by the first two initial time constants. Accordingly, the three-state conformational model of the VSD voltage-sensing response might be refined by including additional

small time- and voltage-dependent structural rearrangements tracked by the FP reporter, as suggested by this study.

Readouts of Neuronal Activity by VSFP3.1_mOrange2

The challenge to develop a fluorescent membrane protein suitable for high-fidelity monitoring of synaptic and action potentials requires knowledge about the biophysical basis of the function of a lead scaffold. Our previous analysis based on a computational modeling approach revealed the significance of several critical features for a suitable voltage-sensitive fluorescent protein including dynamic range, $V_{1/2}$, response kinetics, and fraction of total measured fluorescence attributed to the probe targeted to the membranes of interest (Akemann et al., 2009). The need for minimizing background fluorescence along with kinetic constraints led us to explore the present series of red-shifted FPs in combination with the VSFP3.1 scaffold. As discussed above, analysis of this series yielded valuable reverse engineering insights. To benchmark the present advance in terms of future neurophysiological applications, we evaluated the performance of VSFP3.1_mOrange2 in primary cultured neurons. This promising new VSFP3.1 variant could not only report spontaneous electrical activity with single-cell resolution but also provided reliable readouts without temporal signal averaging. Furthermore, imaging with a CCD camera highlighted the potential of fluorescent protein-based voltage probes for noninvasive and simultaneous recordings of electrical activity from populations of genetically identified neurons. These benchmarking experiments on probing neuronal signals were conducted in monolayer cell cultures. Characterization of corresponding optical signals from brain slices or living animals will nevertheless require additional efforts. At present, we do not see any reason why we would not expect useful optical signals from at least synchronizing cell assemblies embedded in intact tissue. We expect that, along with the possibility of genetically targeting these probes to specific cell populations, an optical report of neuronal activities even without resolving single cells will provide a powerful complement to optical imaging modalities that are already used for physiological experiments in vitro and in vivo.

From the perspective of probe development, this current work constitutes an important advance in the development of optical sensors for electrical signals of neurons and provides valuable insights into our understanding of the voltage-sensing mechanism related to the VSD of Ci-VSP.

SIGNIFICANCE

Significant progress in our understanding of neuronal network dynamics underlying brain function requires the ability to monitor the activity of a large number of neurons simultaneously. Optical methods based on fluorescent probes can provide a methodological solution to this problem. More recently, genetically encoded probes have been designed to target specific cell types. Among this class of probes, voltage-sensitive reporter proteins have been particularly desired but also challenging to develop. By using a reverse engineering approach based on fluorescent proteins with optimized photophysical and biochemical properties, we shed light on the voltage-sensing mechanism of VSFP3.1, the genetically encoded voltage reporter with

the fastest fluorescence response kinetics reported to date. Further development of this probe resulted in a novel red-shifted voltage reporter protein (VSFP3.1_mOrange2) that allowed for reliable optical readouts of spontaneous electrical signals in hippocampal neurons. This current work not only constitutes an important advance in the development of optical sensors for neuronal circuit activity but also provides valuable insights into our understanding of the voltage-sensing mechanism of Ci-VSP (*Ciona intestinalis* voltage sensor-containing phosphatase). This family of red-shifted voltage-sensitive fluorescent proteins will facilitate experimental approaches directed toward the characterization of neuronal network dynamics and information processing in the brain.

EXPERIMENTAL PROCEDURES

Construction of VSFP3.1 Spectral Variants

Citrine and mOrange2 were kind gifts from O. Griesbeck (Max Planck Institute of Neurobiology) and R.Y. Tsien (University of California), respectively. The cDNA coding for TagRFP and mKate2 were provided by D.M. Chudakov (Shemyakin-Ovchinnikov Institute of Bioorganic Chemistry) and are commercially available (Evrogen). VSFP3.1 variants were generated by first amplifying the coding sequence of Citrine, mOrange2, TagRFP, and mKate2 by using different sets of sense and antisense primers comprising a NotI and HindIII site, respectively. A GFP-like N-terminal end was also encoded within the sense primers to increase the tolerance to protein fusion (Shaner et al., 2004). VSFP3.1_Citrine, VSFP3.1_mOrange2, VSFP3.1_TagRFP, and VSFP3.1_mKate2 were then obtained by substituting Cerulean in VSFP3.1 with the amplified PCR fragments mentioned above by using NotI and HindIII restriction endonucleases (New England Biolabs). The R217Q mutation was introduced by site-directed mutagenesis using high-fidelity PCR (PfuTurbo polymerase; Stratagene). The VSFP3.1_mOrange2(Q217R) construct was obtained by subcloning mOrange2 into VSFP2A (Dimitrov et al., 2007) following digestion with NotI and HindIII restriction enzymes. VSFP3.1_mCitrine, VSFP3.1_mOrange2, VSFP3.1_TagRFP, and VSFP3.1_mKate2 were subsequently subcloned into pEF1-Myc-HisA vector (kind gift from T. Shimogori, RIKEN Brain Science Institute) for expression in primary cultures. All constructs were confirmed by sequence analysis.

Cell Culture and Transfection

PC12 cells were grown in Dulbecco's modified Eagle's medium supplemented with a mixture of 5% fetal calf serum/10% horse serum and plated onto poly-D-lysine-coated coverslips. Transfections were carried out 24 hr after plating using Lipofectamine 2000 transfection reagent (Invitrogen) according to the manufacturer's instructions. Primary cultures of hippocampal neurons were prepared from E18 mouse embryos. The dissociated cells were plated on coverslips precoated with poly-D-lysine/poly-L-ornithine and maintained in neurobasal medium supplemented with 3.9 mM L-glutamine, 1% B-27, 1.5% horse serum, and 25% conditioned medium (Sumitomo). Cells were transfected 6 days after plating using Lipofectamine 2000 transfection reagent. Experiments with PC12 cells and hippocampal neurons were performed 48 hr and 8–9 days after transfection, respectively. Confocal laser scanning microscopy was performed using the C1 spectral imaging system (Eclipse C1Si, Nikon) equipped with 40× (NA 0.75) and 60× (NA 0.85) water immersion objectives. Imaging was carried out using a 440 nm diode laser (VSFP3.1), a 488 nm argon laser (VSFP3.1_Citrine), or a 543 nm He-Ne laser (VSFP3.1_mOrange2/VSFP3.1_TagRFP/VSFP3.1_mKate2). Fluorescence images were processed using Image-Pro 6.0 software.

Optical Imaging and Electrophysiology

Coverslips with transfected cells were placed in a recording chamber mounted on the stage of an inverted microscope (Eclipse TE2000-U, Nikon), and whole-cell voltage-clamp recordings were performed using an Axopatch 200B amplifier (Axon Instruments). Borosilicate glass electrodes of a resistance of

3–5 MΩ were pulled on a two-stage vertical puller (PP-830, Narishige). Recordings were performed in a perfused chamber at 35°C. For PC12 cells, the pipette solution contained 130 mM CsCl, 1 mM MgCl$_2$, 20 mM HEPES, 5 mM EGTA, 3 mM MgATP (pH 7.2). The external solution contained 150 mM NaCl, 4 mM KCl, 2 mM CaCl$_2$, 1 mM MgCl$_2$, 5 mM glucose, 5 mM HEPES. For primary hippocampal cultures, the pipette solution contained 60 mM K gluconate, 60 mM K methanesulfonate, 20 mM KCl, 3 mM MgCl$_2$, 4 mM Na$_2$ATP, 0.4 mM NaGTP, 15 mM HEPES, 2 mM EGTA, 0.8 mM CaCl$_2$ (pH 7.4). The external solution contained 140 mM NaCl, 3 mM KCl, 3 mM CaCl$_2$, 1 mM MgSO$_4$, 0.5 mM Na$_2$HPO$_4$, 10 mM glucose, 10 mM HEPES. Fluorescence transients were acquired using a photodiode-based photometry system (TILL Photonics) and a cooled charge-coupled device (CCD) camera (Sensicam, PCO). Clampex software (Axon Instruments) was used for data acquisition, synchronization of voltage command pulses, and fluorescence excitation. Fluorescence was induced by light from a computer-controlled monochromator (Polychrome V, TILL Photonics). Optical filter sets: VSFP3.1_Cerulean (ex 440): 465 longpass (LP) dichroic and 480LP; VSFP3.1_Citrine (ex 490): 506LP dichroic and 514LP; VSFP3.1_mOrange2 (ex 540): 560LP dichroic and 568LP; VSFP3.1_TagRFP (ex 540): 560LP dichroic and 568LP; VSFP3.1_mKate2 (ex 565): 585LP dichroic and 630/30 bandpass. The fluorescence and electrophysiological signals were analyzed using Clampfit (Axon Instruments) and Origin software (OriginLab). Background fluorescence was corrected by subtracting offsets measured from regions devoid of cells. Photobleaching was corrected by division of a double exponential fit of the fluorescence trace at constant membrane voltage. ΔF/F values as a function of step voltage (Vm) were fitted with a Boltzmann function [$\Delta F/F = A + (D - A)/(1 + \exp((V_m - V_{1/2})/s))$], yielding voltage of half-maximal response ($V_{1/2}$) and dynamic range (D). Parameters A and s are voltage-independent offset and a slope factor, respectively.

SUPPLEMENTAL DATA

Supplemental Data include six figures and one table and can be found with this article online at http://www.cell.com/chemistry-biology/supplemental/S1074-5521(09)00406-2.

REFERENCES

Akemann, W., Lundby, A., Mutoh, H., and Knöpfel, T. (2009). Effect of voltage sensitive fluorescent proteins on neuronal excitability. Biophys. J. 96, 3959–3976.

Akerboom, J., Rivera, J.D., Guilbe, M.M., Malave, E.C., Hernandez, H.H., Tian, L., Hires, S.A., Marvin, J.S., Looger, L.L., and Schreiter, E.R. (2009). Crystal structures of the GCaMP calcium sensor reveal the mechanism of fluorescence signal change and aid rational design. J. Biol. Chem. 284, 6455–6464.

Ataka, K., and Pieribone, V.A. (2002). A genetically targetable fluorescent probe of channel gating with rapid kinetics. Biophys. J. 82, 509–516.

Baird, G.S., Zacharias, D.A., and Tsien, R.Y. (1999). Circular permutation and receptor insertion within green fluorescent proteins. Proc. Natl. Acad. Sci. USA 96, 11241–11246.

Borst, J.W., Hink, M.A., van Hoek, A., and Visser, A.J. (2005). Effects of refractive index and viscosity on fluorescence and anisotropy decays of enhanced cyan and yellow fluorescent proteins. J. Fluoresc. 15, 153–160.

Buzsaki, G. (2004). Large-scale recording of neuronal ensembles. Nat. Neurosci. 7, 446–451.

Buzsaki, G., and Draguhn, A. (2004). Neuronal oscillations in cortical networks. Science 304, 1926–1929.

Campbell, R.E., Tour, O., Palmer, A.E., Steinbach, P.A., Baird, G.S., Zacharias, D.A., and Tsien, R.Y. (2002). A monomeric red fluorescent protein. Proc. Natl. Acad. Sci. USA 99, 7877–7882.

Cevc, G. (1990). Membrane electrostatics. Biochim. Biophys. Acta 1031, 311–382.

Cha, A., and Bezanilla, F. (1997). Characterizing voltage-dependent conformational changes in the Shaker K$^+$ channel with fluorescence. Neuron 19, 1127–1140.

Cohen, E., Ivenshitz, M., Amor-Baroukh, V., Greenberger, V., and Segal, M. (2008). Determinants of spontaneous activity in networks of cultured hippocampus. Brain Res. 1235, 21–30.

Cossart, R., Lkegaya, Y., and Yuste, R. (2005). Calcium imaging of cortical networks dynamics. Cell Calcium 37, 451–457.

Crochet, S., and Petersen, C.C. (2006). Correlating whisker behavior with membrane potential in barrel cortex of awake mice. Nat. Neurosci. 9, 608–610.

Dimitrov, D., He, Y., Mutoh, H., Baker, B.J., Cohen, L., Akemann, W., and Knöpfel, T. (2007). Engineering and characterization of an enhanced fluorescent protein voltage sensor. PLoS ONE 2, e440.

Griesbeck, O., Baird, G.S., Campbell, R.E., Zacharias, D.A., and Tsien, R.Y. (2001). Reducing the environmental sensitivity of yellow fluorescent protein. J. Biol. Chem. 276, 29188–29194.

Kneen, M., Farinas, J., Li, Y., and Verkman, A.S. (1998). Green fluorescent protein as a noninvasive intracellular pH indicator. Biophys. J. 74, 1591–1599.

Knöpfel, T., Diez-Garcia, J., and Akemann, W. (2006). Optical probing of neuronal circuit dynamics: genetically encoded versus classical fluorescent sensors. Trends Neurosci. 29, 160–166.

Kohout, S.C., Ulbrich, M.H., Bell, S.C., and Isacoff, E.Y. (2008). Subunit organization and functional transitions in Ci-VSP. Nat. Struct. Mol. Biol. 15, 106–108.

Llopis, J., McCaffery, J.M., Miyawaki, A., Farquhar, M.G., and Tsien, R.Y. (1998). Measurement of cytosolic, mitochondrial, and Golgi pH in single living cells with green fluorescent proteins. Proc. Natl. Acad. Sci. USA 95, 6803–6808.

Lundby, A., Mutoh, H., Dimitrov, D., Akemann, W., and Knöpfel, T. (2008). Engineering of a genetically encodable fluorescent voltage sensor exploiting fast Ci-VSP voltage-sensing movements. PLoS ONE 3, e2514.

Manns, I.D., Sakmann, B., and Brecht, M. (2004). Sub- and suprathreshold receptive field properties of pyramidal neurones in layers 5A and 5B of rat somatosensory barrel cortex. J. Physiol. 556, 601–622.

Mannuzzu, L.M., Moronne, M.M., and Isacoff, E.Y. (1996). Direct physical measure of conformational rearrangement underlying potassium channel gating. Science 271, 213–216.

Merzlyak, E.M., Goedhart, J., Shcherbo, D., Bulina, M.E., Shcheglov, A.S., Fradkov, A.F., Gaintzeva, A., Lukyanov, K.A., Lukyanov, S., Gadella, T.W., and Chudakov, D.M. (2007). Bright monomeric red fluorescent protein with an extended fluorescence lifetime. Nat. Methods 4, 555–557.

Murata, Y., Iwasaki, H., Sasaki, M., Inaba, K., and Okamura, Y. (2005). Phosphoinositide phosphatase activity coupled to an intrinsic voltage sensor. Nature 435, 1239–1243.

Mutoh, H., Perron, A., Dimitrov, D., Iwamoto, Y., Akemann, W., Chudakov, D.M., and Knöpfel, T. (2009). Spectrally-resolved response properties of the three most advanced FRET based fluorescent protein voltage probes. PLoS ONE 4, e4555.

Nagai, T., Sawano, A., Park, E.S., and Miyawaki, A. (2001). Circularly permuted green fluorescent proteins engineered to sense Ca^{2+}. Proc. Natl. Acad. Sci. USA 98, 3197–3202.

Nakai, J., Ohkura, M., and Imoto, K. (2001). A high signal-to-noise Ca^{2+} probe composed of a single green fluorescent protein. Nat. Biotechnol. *19*, 137–141.

Pakhomov, A.A., and Martynov, V.I. (2008). GFP family: structural insights into spectral tuning. Chem. Biol. *15*, 755–764.

Perron, A., Mutoh, H., Akemann, W., Gautam, S.G., Dimitrov, D., Iwamoto, Y., and Knöpfel, T. (2009). Second and third generation voltage-sensitive fluorescent proteins for monitoring membrane potential. Front. Mol. Neurosci. *2*, 5.

Sakai, R., Repunte-Canonigo, V., Raj, C.D., and Knöpfel, T. (2001). Design and characterization of a DNA-encoded, voltage-sensitive fluorescent protein. Eur. J. Neurosci. *13*, 2314–2318.

Shaner, N.C., Campbell, R.E., Steinbach, P.A., Giepmans, B.N., Palmer, A.E., and Tsien, R.Y. (2004). Improved monomeric red, orange and yellow fluorescent proteins derived from *Discosoma* sp. red fluorescent protein. Nat. Biotechnol. *22*, 1567–1572.

Shaner, N.C., Steinbach, P.A., and Tsien, R.Y. (2005). A guide to choosing fluorescent proteins. Nat. Methods *2*, 905–909.

Shaner, N.C., Patterson, G.H., and Davidson, M.W. (2007). Advances in fluorescent protein technology. J. Cell Sci. *120*, 4247–4260.

Shaner, N.C., Lin, M.Z., McKeown, M.R., Steinbach, P.A., Hazelwood, K.L., Davidson, M.W., and Tsien, R.Y. (2008). Improving the photostability of bright monomeric orange and red fluorescent proteins. Nat. Methods *5*, 545–551.

Shcherbo, D., Merzlyak, E.M., Chepurnykh, T.V., Fradkov, A.F., Ermakova, G.V., Solovieva, E.A., Lukyanov, K.A., Bogdanova, E.A., Zaraisky, A.G., Lukyanov, S., and Chudakov, D.M. (2007). Bright far-red fluorescent protein for whole-body imaging. Nat. Methods *4*, 741–746.

Shcherbo, D., Murphy, C.S., Ermakova, G.V., Solovieva, E.A., Chepurnykh, T.V., Shcheglov, A.S., Verkhusha, V.V., Pletnev, V.Z., Hazelwood, K.L., Roche, P.M., et al. (2009). Far-red fluorescent tags for protein imaging in living tissues. Biochem. J. *418*, 567–574.

Siegel, M.S., and Isacoff, E.Y. (1997). A genetically encoded optical probe of membrane voltage. Neuron *19*, 735–741.

Souslova, E.A., Belousov, V.V., Lock, J.G., Stromblad, S., Kasparov, S., Bolshakov, A.P., Pinelis, V.G., Labas, Y.A., Lukyanov, S., Mayr, L.M., and Chudakov, D.M. (2007). Single fluorescent protein-based Ca^{2+} sensors with increased dynamic range. BMC Biotechnol. *7*, 37.

Suhling, K., Siegel, J., Phillips, D., French, P.M., Leveque-Fort, S., Webb, S.E., and Davis, D.M. (2002). Imaging the environment of green fluorescent protein. Biophys. J. *83*, 3589–3595.

Tsutsui, H., Karasawa, S., Okamura, Y., and Miyawaki, A. (2008). Improving membrane voltage measurements using FRET with new fluorescent proteins. Nat. Methods *5*, 683–685.

Uskova, M.A., Borst, J.W., Hink, M.A., van Hoek, A., Schots, A., Klyachko, N.L., and Visser, A.J. (2000). Fluorescence dynamics of green fluorescent protein in AOT reversed micelles. Biophys. Chem. *87*, 73–84.

van Manen, H.J., Verkuijlen, P., Wittendorp, P., Subramaniam, V., van den Berg, T.K., Roos, D., and Otto, C. (2008). Refractive index sensing of green fluorescent proteins in living cells using fluorescence lifetime imaging microscopy. Biophys. J. *94*, L67–L69.

Verkhusha, V.V., and Lukyanov, K.A. (2004). The molecular properties and applications of Anthozoa fluorescent proteins and chromoproteins. Nat. Biotechnol. *22*, 289–296.

Verkhusha, V.V., Pozhitkov, A.E., Smirnov, S.A., Borst, J.W., van Hoek, A., Klyachko, N.L., Levashov, A.V., and Visser, A.J. (2003). Effect of high pressure and reversed micelles on the fluorescent proteins. Biochim. Biophys. Acta *1622*, 192–195.

Villalba-Galea, C.A., Sandtner, W., Starace, D.M., and Bezanilla, F. (2008). S4-based voltage sensors have three major conformations. Proc. Natl. Acad. Sci. USA *105*, 17600–17607.

Villalba-Galea, C.A., Sandtner, W., Dimitrov, D., Mutoh, H., Knöpfel, T., and Bezanilla, F. (2009). Charge movement of a voltage-sensitive fluorescent protein. Biophys. J. *96*, L19–L21.